

High-Energy Gamma-Ray Emission in Heavy-Ion Collisions

J. Stevenson, K. B. Beard, W. Benenson, J. Clayton, E. Kashy, A. Lampis, D. J. Morrissey, M. Samuel, R. J. Smith, C. L. Tam, and J. S. Winfield

*National Superconducting Cyclotron Laboratory and Department of Physics and Astronomy,
Michigan State University, East Lansing, Michigan 48824*

(Received 6 March 1986)

Energy and angular distributions were measured for high-energy ($E_\gamma > 10$ MeV) gamma rays from collisions of ^{14}N on Pb, Zn, and C at beam energies of $E/A = 20, 30,$ and 40 MeV. The gamma-ray energy spectrum was measured to about 120 MeV at $E/A = 40$ MeV and to about 80 MeV at $E/A = 20$ MeV. For $E_\gamma > 20$ MeV the spectra are roughly exponential with characteristic slope parameters ranging from 10.0 MeV for $^{14}\text{N} + \text{Pb}$ at $E/A = 20$ MeV to 14.2 MeV at $E/A = 40$ MeV. Reasonable agreement is obtained with a model employing bremsstrahlung from individual neutron-proton collisions in the heavy-ion collision.

PACS numbers: 25.70.-z

Unexpectedly large yields of high-energy gamma rays are produced in heavy-ion collisions at intermediate energies.^{1,2} For example, in a recent experiment¹ the cross section of gamma rays with energies above 10 MeV was shown to be about 0.5 mb for $^{14}\text{N} + \text{Cu}$ at $E/A = 40$ MeV, and it was demonstrated that the energy spectrum extends to energies above 100 MeV.

No theoretical model seemed to explain these results. One suggested mechanism was coherent bremsstrahlung³⁻⁶ due to the sudden deceleration of the projectile in the collision, which would mean that high-energy gamma rays could be used to study the dynamics of the collision process. However, the measured angular distribution is inconsistent with the predicted quadrupole shape of the coherent bremsstrahlung model. The early data of Beard *et al.*¹ covered a limited angular range (0° to 40° , in the laboratory) and were for a stopping target, but they demonstrated that the high-energy gamma-ray angular distribution is fairly isotropic. Bremsstrahlung calculations carried out in a cascade model by Ko, Bertsch, and Aichelin⁵ indicated that bremsstrahlung of projectile and target nucleons would dominate over coherent nucleus-nucleus bremsstrahlung for light ($Z < 20$) systems because of the strength of the dipole radiation from neutron-proton collisions. Their calculations indicated that coherent nucleus-nucleus bremsstrahlung would become dominant for heavier systems as a result of the Z^2 dependence of the gamma-ray yield. The difficulty in ascribing the high-energy gamma-ray yield to the nucleon-nucleon part of the bremsstrahlung process was that the predicted energy spectrum has the characteristic $1/E$ form while the observed spectrum was exponential. If the gamma rays do not come from a coherent process, they may be created during the later stages of the collision under conditions that nearly approach statistical equilibrium.

Since Ref. 1 is the only published experimental work

in this field, more detailed measurements over a full range of angles, targets, and beam energies are needed to discriminate between the various possible mechanisms. We report here high-energy gamma-ray measurements carried out with ^{14}N beams of $E/A = 20, 30,$ and 40 MeV from the K500 Cyclotron of the National Superconducting Cyclotron Laboratory. Gamma-ray energy spectra were measured at 30° intervals from 30° to 150° for carbon, zinc, and lead targets.

The measurements were made with two gamma-ray telescopes, each of which consisted of an active CsI scintillator gamma-ray converter ($\gamma \rightarrow e^+ + e^-$) followed by an eight-element Cherenkov-detector range stack. The plastic Cherenkov detectors were made of Bicron BC-480, which consists of Lucite with a wave-shifter additive for improved light collection and uniformity. The first and second Cherenkov detectors were 1.27 and 2.54 cm thick, and the remaining six detectors were each 5.08 cm thick. The light collection, with two photomultiplier tubes, was sufficient to resolve the signal due to one electron from that due to a pair. Therefore it was possible to determine the ranges of the electron and positron, separately. The gamma-ray energy was deduced from these ranges. Cherenkov-based gamma-ray detectors are insensitive to most heavy-ion-collision products such as protons and neutrons. The detectors can thus operate with high beam intensities and thick targets [5 nA (particle) and 50 mg/cm², respectively, in the present experiment]. The most serious background for this measurement was cosmic-ray muons which gave a count rate of about 0.5 count/s. This background was reduced to about 16 counts/h by enclosing the detector on the front, top, and sides with an anticoincidence shield. The front shield was a plastic Cherenkov detector, and the top and sides were plastic scintillators. Time of flight relative to the rf of the cyclotron was recorded for each event. This information showed

that the neutron-induced events corresponded to gamma rays below the energies of interest in this paper, and that 80% of the remaining muons were eliminated with this information.

The gamma-ray detectors were operated with their converters at 0.5 m from the target, and each subtended 40 msr. The detectors were used in tandem, one for 30°, 60°, and 90° and the other for 90°, 120°, and 150°. A 0.32-cm-thick CsI crystal with a pair-conversion efficiency ranging from 5% at 20 MeV to 10% at 100 MeV was used in the forward-angle detector. The backward-angle detector used a 0.64-cm-thick CsI crystal. The responses of individual Cherenkov elements were equalized with muons required to go through the converter and a scintillator at the back of the detector telescope. The efficiency and resolution of the detectors were simulated with a Monte Carlo calculation. The main ingredients are the pair-production cross section of gammas as a function of energy⁷ and the range-energy relations.⁸ The present data are in excellent agreement in spectral shape with those of Nifenecker *et al.*⁹ for $^{40}\text{Ar} + \text{Au}$ at $E/A = 30$ MeV, and the agreement in absolute value is also good when the data are scaled for the different target and projectile combinations.

Figure 1 shows the angular distribution of high-energy gamma rays for $E/A = 40$ MeV ^{14}N on lead and carbon targets, for four cuts at $E_\gamma = 20, 40, 60,$ and 80 MeV. The angular distributions are all slightly forward peaked; for example, $\sigma(30^\circ)/\sigma(150^\circ) = 2.4$ for lead

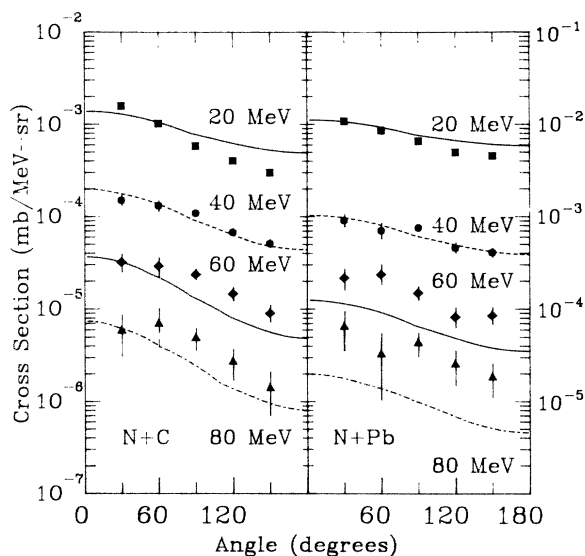


FIG. 1. Plot of the laboratory angular distributions of high-energy gamma rays for $E/A = 40$ MeV $^{14}\text{N} + \text{C}$ and $^{14}\text{N} + \text{Pb}$, at gamma-ray energies of $E_\gamma = 20$ (square), 40 (circle), 60 (diamond), 80 (triangle) MeV. Theoretical curves are thermal bremsstrahlung calculations as described in the text.

and 3.0 for carbon targets at $E_\gamma = 40$ MeV. Similar distributions are observed for all targets and beam energies. These angular distributions are consistent with isotropic emission from a recoiling source with corresponding source velocities (see Table I) closer to the velocity of the nucleon-nucleon center of mass than to the velocity of the nucleus-nucleus center of mass.

The gamma-ray cross section for the lead target is about 7 times larger than that for the carbon target, which corresponds to a roughly $A^{2/3}$ target dependence. For coherent nucleus-nucleus bremsstrahlung a primarily quadrupole angular distribution is expected. Dipole contributions would also occur for projectile-target combinations with different ratios of A/Z such as $^{14}\text{N} + \text{Pb}$, because of the net current in the nucleus-nucleus center-of-mass frame. Small isotropic terms, at high gamma-ray energies, would also be expected as a result of the magnetic-moment interaction.¹⁰ The present data seem to rule out coherent nucleus-nucleus bremsstrahlung as an important mechanism here.

Figure 2 shows the gamma-ray energy spectrum taken at 90° for $^{14}\text{N} + \text{Pb}$ and C at $E/A = 40, 30,$ and 20 MeV. The steeply falling low-energy parts ($E_\gamma < 20$ MeV) have a nearly constant slope parameter ($ae^{-E/\tau}$) of 2 MeV. The data for $E_\gamma > 35$ MeV can be conveniently parametrized in terms of isotropic emission from a recoiling source, with a single exponential energy spectrum of the form $be^{-E/\tau}$. These slope parameters, shown in Table I, are rather similar to those obtained from charged particles for similar reactions although the absolute yields are about three orders of magnitude smaller. Perhaps the most interesting feature of the beam-energy dependence of the gamma-ray spectra is its weakness. High-energy gamma-ray production does not appear to have a

TABLE I. Parameters from the best fit to the high-energy gamma-ray data. Spectra for each target and beam energy were fitted on the assumption of isotropic emission from a recoiling source with velocity β_{exp} with a gamma-ray spectrum of the form $be^{-E/\tau}$. For comparison, $\beta_{NN}^{\text{c.m.}}$ and $\beta_{\text{nuc-nuc}}^{\text{c.m.}}$ are the nucleon-nucleon and nucleus-nucleus center-of-mass velocities for the projectile-target system.

Target	E/A (MeV)	τ (MeV)	β_{exp}	β_{NN}	$\beta_{\text{nuc-nuc}}$
Pb	20	10.0	0.08	0.104	0.013
Pb	30	12.0	0.11	0.127	0.016
Pb	40	14.2	0.10	0.145	0.019
Zn	20	8.3	0.05	0.104	0.037
Zn	30	11.8	0.11	0.127	0.045
Zn	40	13.7	0.10	0.145	0.052
C	20	7.7	0.08	0.104	0.111
C	30	11.1	0.10	0.127	0.135
C	40	13.3	0.12	0.145	0.156

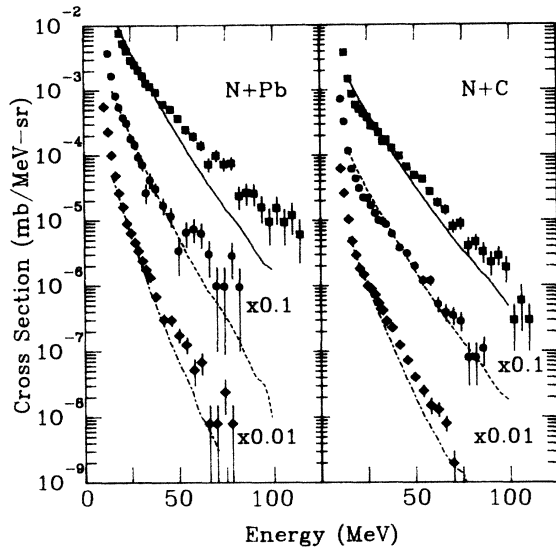


FIG. 2. The gamma-ray energy spectrum measured at 90° for $^{14}\text{N}+\text{Pb}$ and $^{14}\text{N}+\text{C}$ at beam energies $E/A = 40$ (square), 30 (circle), and 20 (diamond) MeV. Theoretical curves are those of the thermal bremsstrahlung model as described in the text.

threshold, at least over the present energy range, nor the steep energy dependence of pion production.¹¹ It is interesting to note that if the gamma-ray energy spectrum is extrapolated to the energy equivalent of the pion mass, the cross sections are quite similar to the pion cross sections. For example the extrapolated cross section of gammas above the π^0 mass for $E/A = 40$ MeV $^{14}\text{N}+\text{Zn}$ is 20 nb, and the π^0 yield for $E/A = 35$ MeV $^{14}\text{N}+\text{Ni}$ is about 60 nb.¹¹ Thus pion and gamma-ray production might well be due to similar processes with the apparent differences in cross sections arising from the pion rest mass and the fine-structure constant.

The curves in Figs. 1 and 2 are based on a model which assumes that the gamma rays are bremsstrahlung from collisions of fast neutrons and protons in a thermal source. The bremsstrahlung yield is calculated in the framework of the nuclear fireball model. The yield per nucleon-nucleon collision of gamma rays above 10 MeV was calculated for an isotropic gas at a given temperature. The bremsstrahlung is determined in the classical long-wavelength approximation.¹² The bremsstrahlung yield was then folded with the predicted fireball formation cross section, size, and temperature to predict the absolute gamma-ray yield. The number of nucleon-nucleon scatterings that a nucleon undergoes was calculated with the assumption of a total path length of a fireball radius, and was typically one to two scatterings. This procedure is not really dependent on the validity of the fireball model as long as it is a good parametrization of the proton and neutron yield in the reaction, and as long as the nucleons

are sufficiently localized in the heavy-ion collision such that they collide with each other. By comparison the incoherent bremsstrahlung mechanism proposed by Ko, Bertsch, and Aichelin⁵ considered only the first scattering of projectile and target nucleons. The difficulty with this model is that the incident projectile nucleons are all at the beam energy (if one neglects Fermi motion). This mechanism only produces gamma rays up to an energy equal to half the beam energy per nucleon and predicts a $1/E$ energy spectrum. The inclusion of Fermi motion into these calculations in the future will shed light on the relative contribution of first-collision production. However, as in the case of pion production, the effect of the Pauli exclusion principle is very important and has to be carefully taken into account. Bremsstrahlung from a hot, isotropic gas gives an essentially exponential gamma-ray energy spectrum with a slope parameter close to the temperature of the gas. A very similar calculation of thermal bremsstrahlung has been performed by Nifenecker and Bondorf¹³ to explain the gamma-ray data of Grosse.²

In conclusion, we have seen that high-energy gamma-ray emission occurs for intermediate-energy heavy-ion reactions from $E/A = 20$ to 40 MeV with no indication of a sharp threshold. The data for all beam energies and targets are slightly forward peaked, which is characteristic of isotropic emission from a recoiling source. The data can be explained in terms of incoherent nucleon-nucleon bremsstrahlung from a thermal source. On the assumption that this mechanism is correct, gamma rays are produced early in the collision when the energetic nucleons are still very localized, but they are not primarily due to first collisions of projectile and target nucleons. The absence of coherent bremsstrahlung is probably a result of the small projectile size, and we plan future experiments with much heavier beams in order to search for this mechanism.

We thank G. Bertsch, U. Mosel, and H. Nifenecker for helpful discussions. This work was supported in part by a grant from the National Science Foundation.

¹K. B. Beard *et al.*, Phys. Rev. C **32**, 1111 (1985).

²E. Grosse, in *Proceedings of the International Workshop on Gross Properties of Nuclei and Nuclear Excitations XIII*, Hirschegg, Austria, 1985, edited by H. Feldmeier (Gesellschaft für Schwerionenforschung und Institut für Kernphysik, Technische Hochschule, Darmstadt, West Germany, 1985).

³J. I. Kapusta, Phys. Rev. C **15**, 1580 (1977).

⁴D. Vasak *et al.*, Nucl. Phys. **A428**, 291 (1984).

⁵Che Ming Ko, G. Bertsch, and J. Aichelin, Phys. Rev. C **31**, 2324 (1985).

⁶W. Bauer, W. Cassing, U. Mosel, M. Tohyama, and R. Y. Cusson, private communication.

⁷J. H. Hubbell, H. A. Gimm, and I. Overbo, *J. Phys. Chem. Ref. Data* **9**, 1023 (1980).

⁸M. J. Berger and S. M. Seltzer, National Bureau of Standards Report No. NBSIR 82-2550-A, 1983 (unpublished).

⁹H. Nifenecker *et al.*, in Proceedings of the Twenty-Fourth International Winter Meeting on Nuclear Physics, Bormio, Italy, 1986 (to be published).

¹⁰U. Mosel, in Ref. 9.

¹¹P. Braun-Munzinger *et al.*, *Phys. Rev. Lett.* **52**, 255 (1984).

¹²J. D. Jackson, *Classical Electrodynamics* (Wiley, New York, 1962).

¹³H. Nifenecker and J. P. Bondorf, *Nucl. Phys.* **A442**, 478 (1985).